RESEARCH/REVIEW ARTICLE

Ice volume changes (1936–1990–2007) and ground-penetrating radar studies of Ariebreen, Hornsund, Spitsbergen

Javier Lapazaran,[1] Michal Petlicki,[2] Francisco Navarro,[1] Francisco Machío,[3] Darek Puczko,[4] Piotr Glowacki[4] & Adam Nawrot[4]

[1] Department of Mathematics Applied to Information Technology, School of Telecommunications Engineering, Technical University of Madrid, Av. Complutense, 30, Ciudad Universitaria, ES-28040 Madrid, Spain
[2] Center for Advanced Studies in Arid Zones, P.O. Box 554, Raúl Bitrán s/n, La Serena, Chile
[3] Higher University College of Engineering and Architecture of the Pontifical University of Salamanca in Madrid, Paseo Juan XXIII, 3, ES-28040 Madrid, Spain
[4] Institute of Geophysics, Polish Academy of Sciences, ul. Księcia Janusza 64, PL-01-452 Warsaw, Poland

Keywords
Ice-volume changes; ground-penetrating radar; thinning rate; Ariebreen; Spitsbergen; Svalbard.

Correspondence
Javier Lapazaran, Department of Mathematics Applied to Information Technology, School of Telecommunications Engineering, Technical University of Madrid, Av. Complutense, 30, Ciudad Universitaria, ES-28040 Madrid, Spain.
E-mail: javier.lapazaran@upm.es

Abstract

Ariebreen is a small (0.37 km^2)-valley glacier located in southern Spitsbergen. Our ground-penetrating radar surveys of the glacier show that it is less than 30 m thick on average, with a maximum thickness of 82 m, and it appears to be entirely cold. By analysing digital terrain models of the ice surface from different dates, we determine the area and volume changes during two periods, 1936–1990 and 1990–2007. The total ice volume of the glacier has decreased by 73% during the entire period 1936–2007, which is equivalent to a mean mass balance rate of -0.61 ± 0.17 m y^{-1} w.eq. The glacier thinning rate has increased markedly between the first and second periods, from -0.50 ± 0.22 to -0.95 ± 0.17 m y^{-1} w.eq.

To access the supplementary material for this article, please see Supplementary files under Article Tools online.

Most Svalbard glaciers have experienced a significant recession since at least the 1930s, and most likely since the end of Little Ice Age in the early part of the 20th century (Werner 1993). This recession has manifested as thinning and retreating of glacier tongues, though a simultaneous thickening at the uppermost elevations has been reported at many locations (Bamber et al. 2004; Nuth et al. 2007). Moreover, the thinning rate of western Svalbard glaciers has increased during the most recent decades (Kohler et al. 2007).

Ariebreen (77° 01′N, 15° 29′E) is a small-valley glacier (0.37 km^2 in August 2007) located in Wedel Jarlsberg Land, Spitsbergen, Svalbard, ca. 2.5 km to the north-west of Hornsund Polish Polar Station (Fig. 1). The head of the glacier faces east, whereas the tongue of the glacier faces south. The surface of Ariebreen is steep (mean value of about 15°, with local values up to 30°) and the glacier tongue is well exposed to solar radiation as compared to the upper cirque zone. It is of interest to analyse the evolution of Ariebreen under a changing climate because there are many of such small glaciers in Svalbard (Hagen et al. 1993), and their response times to climate changes are expected to be short because of their limited thickness (Cuffey & Paterson 2010). Accordingly, we aim to quantify the mass changes of Ariebreen from analysis of digital terrain models (DTMs) for the years 1936, 1990 and 2007, constructed from aerial photographs and geodetic measurements, and to verify whether its mass loss has accelerated during the recent decades.

Most glaciers investigated in the Hornsund area are known to be polythermal, such as Hansbreen and Werenskioldbreen (Pälli et al. 2003). The small size of Ariebreen, however, might suggest that it is a cold glacier, although it was previously classified as polythermal (Jania

Citation: *Polar Research* 2013, *32*, 11068, http://dx.doi.org/10.3402/polar.v32i0.11068

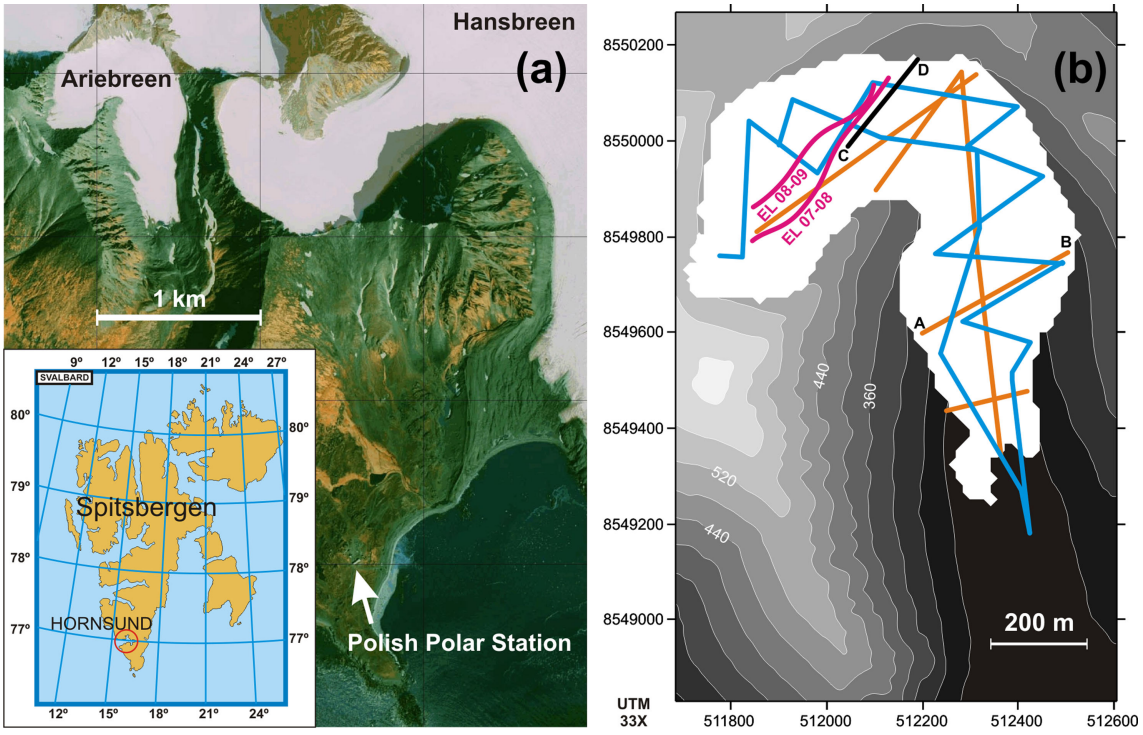

Fig. 1 Location of Ariebreen in the Hornsund region on the island of Spitsbergen, Svalbard. The orthophotograph in (a) corresponds to 1990 (Jania et al. 2002; Kolondra 2002), while the glacier extent depicted in (b) corresponds to 2007. In (b) the layout of the 200-MHz radar profiles done in August 2006 (orange lines), and the 25-MHz profiles done in April 2007 (blue lines) and April 2009 (black line) are shown. The radar sections corresponding to profiles A–B and C–D are shown in Fig. 5. The equilibrium line (EL) at the end of the balance years 2007–08 and 2008–09 is also shown. The corresponding accumulation area ratios were 0.25 and 0.20.

1988). We aim to verify, from ground-penetrating radar (GPR) data, whether Ariebreen is cold or polythermal as this may be important for the erosional capacity and the suspended sediment load of the Ariebekken river. This water discharge stream from Ariebreen flows out of Ariedalen valley to Revdalen valley through a wide delta, where biological and geomorphological studies have been conducted for 50 years (e.g., Kuziemski 1968), hence the interest to characterize the hydrothermal regime of the glacier.

Data and methods

We estimated the present ice volume from GPR ice thickness data, and calculated ice volume changes from surface elevation changes by differencing DTMs. In this section, we describe the GPR measurements and how each DTM was created, and then discuss the planar area, total volume, volume change and mass balance computations by the geodetic method, with their error estimates. As a rule, we will use the terms "bias" and "error" to refer to the mean value and the standard deviation of the random variable error, respectively. As the bias represents a systematic error, we apply bias correction and take the standard deviation as an error estimate.

Radar surveys and data processing

During the summer of 2006 and the springs of 2007 and 2009, we carried out radar profiles covering the entire surface of Ariebreen (Fig. 1). The total length of profiles was 6400 m (2200 m in 2006, 4000 m in 2007 and 200 m in 2009). The radar data were acquired using a Malå Ramac GPR system (Malå Geoscience, Malå, Sweden) with unshielded antennae of 200 MHz (2006) and of 25 MHz (2007 and 2009). The antennae configuration was collinear following the profile direction (parallel end-fire) in all cases. The 200-MHz antennae were chosen to obtain a higher resolution, in order to detect not only the glacier bed, but also the extent and thickness of the firn layer. The recommended equipment settings for working at 200 MHz limited the maximum depth sampled to about 40 m. Consequently, the bedrock was not reached in the areas of thickest ice. Using the 25-MHz antennae, the bedrock was detected in all cases.

Citation: *Polar Research* 2013, *32*, 11068, http://dx.doi.org/10.3402/polar.v32i0.11068

There have not been radio-wave velocity (RWV) measurements on Ariebreen, but estimates from many common midpoint (CMP) measurements at the neighbouring Hansbreen glacier (Jania et al. 2005) are available, for both spring and summer periods, and both cold and temperate ice. From their results, we apply a RWV of 168 m μs^{-1}, typical of cold ice. At the frequencies of the GPR antennae used, this implies a theoretical range (vertical) resolution of the radar data of 1.68 m for the 25-MHz antennae, and 0.21 m for the 200-MHz antennae, considering the range resolution as one quarter of the wavelength in ice. The range resolution provides a lower bound of the error in thickness. The total error in thickness depends on many factors and will be larger, as explained later. The processing of radar data included band-pass filtering, amplitude scaling, deconvolution, migration where required and conversion to depth using the above RWV.

Digital terrain models

The DTMs of Ariebreen's surface elevation in different years have been constructed interpolating each year's elevation data at the nodes of a common grid. We used as the reference common grid that of the 1990 DTM, which was already available in gridded format (Jania et al. 2002; Kolondra 2002) and therefore did not require interpolation.

For estimating the error in elevation of any of our DTMs, $\varepsilon_{z\ \mathrm{DTM}}$, we considered the contributions of both the error in the data points from which the DTM was constructed, $\varepsilon_{z\ \mathrm{data}}$, and the surface interpolation error inherent to the generation of the DTM from such data points, $\varepsilon_{z\ \mathrm{interp}}$. We assume that these errors are independent, so $\varepsilon_{z\ \mathrm{DTM}}$ can be estimated through the root of the squared summation of $\varepsilon_{z\ \mathrm{data}}$ and $\varepsilon_{z\ \mathrm{interp}}$.

1936 DTM. We constructed the 1936 DTM from sheet B12 (Torellbreen, Spitsbergen) of the 1:100 000 Svalbard topographic map (Norwegian Polar Institute 1953), which is a photogrammetric compilation from oblique aerial photographs taken in 1936. The original map uses the European Datum 1950 (ED50), which we transformed to the WGS-1984 datum within UTM projection (Zone 33X). We digitized the glacier surface elevation from the map contour lines. We also digitized the glacier boundary data points from the map, but extracted their vertical coordinates from the more precise 1990 DTM, which was also used for the ice-free areas. We then interpolated the glacier boundary and surface elevation points to a 20 m × 20 m regular grid using ESRI ArcGIS 9.3 tool Topo2Raster, which is based on the ANUDEM algorithm (version 4.6.3) developed by Hutchinson (1989).

The errors in the 1936 DTM are large because of the uncertainties inherent to the original map, due to the photogrammetric techniques on oblique aerial photographs, and the poor coverage of the source data, limited to the glacier boundary and a few contour lines. To quantify a possible bias in the 1936 map, we compared the map elevations of three ice-free points with slopes lower than 20° in the neighbourhood of Ariebreen, with our own measurements by a differential carrier-phase global positioning system instrument (GPS). We corrected the 1936 DTM with the resulting bias of -6.09 ± 4.23 m, which is very close to the systematic bias in map elevations between the 1990 and 1936 maps obtained by Nuth et al. (2007) for Wedel Jarlsberg Land (-6.50 ± 12.49 m).

In the case of our 1936 DTM, we took as interpolation error the standard deviation of the residuals directly provided by the Topo2Raster routine of ArcGIS software, $\varepsilon_{z\ \mathrm{interp}} = 5.39$ m, and, as a conservative estimate for $\varepsilon_{z\ \mathrm{data}}$, we took Nuth et al.'s (2007) regional value of 12.49 m, giving $\varepsilon_{z\ 1936\ \mathrm{DTM}} = 13.60$ m.

1990 DTM. Our 1990 DTM (20-m resolution) for Ariebreen surface and Ariedalen valley is derived from vertical aerial photographs taken on 12 August 1990 (Jania et al. 2002; Kolondra 2002). The aerial triangulation was based on seven ground control points surveyed by differential carrier-phase GPS in 1995. The vertical accuracy for the glacierized areas of the original 1990 DTM was estimated by its author to be within 2.0–3.0 m (Kolondra, pers. comm. 2010) and therefore we took $\varepsilon_{z\ 1990\ \mathrm{DTM}} = 3.0$ m as a conservative error estimate.

2007 DTM. The 2007 DTM of Ariebreen is based on our own geodetic measurements made on 27 and 29 August 2007, when most of the glacier surface was snow-free. We surveyed the ice surface elevation and the glacier boundary of Ariebreen using a Leica TCR-1105 total station (Leica Geosystems, Heerbrugg, Switzerland). A total of 646 points were measured, of which 192 corresponded to the glacier boundary. The UTM coordinates were computed using Geonet software (Geonet w/2002/2.2). The 2007 DTM was generated using the Kriging method on the same regular grid 20 m × 20 m used in 1936 and 1990 DTMs, getting $\varepsilon_{z\ \mathrm{interp}} = 0.90$ m as standard deviation of the residuals of the cross-validation process. The residual at each data point is evaluated as the difference between the actual data value, and the interpolated value (at this point) obtained using the remaining data points. The vertical precision of the

original data points was better than 0.01 m, but, to take into account the uncertainties associated with the thin snow layer on the accumulation area or other surface irregularities, we assume a conservative value for $\varepsilon_{z\ \mathrm{data}} = 0.50$ m. The root of the squared summation of $\varepsilon_{z\ \mathrm{interp}}$ and $\varepsilon_{z\ \mathrm{data}}$ gives $\varepsilon_{z\ 2007\ \mathrm{DTM}} = 1.03$ m.

Ice thickness (2007), bedrock topography and glacier elevation change maps

Ice thickness (2007) and subglacial bedrock maps. The ice thickness map was constructed from our radar data, using 461 ice thickness data points picked from the radargrams and 192 zero-thickness data points corresponding to the glacier boundary. The ice thickness points corresponded to two different campaigns, done at the end of a summer and the beginning of the subsequent spring. The difference in ice thickness at the crossover points of the radar profiles from different campaigns was used to estimate any possible bias. We detected a bias equivalent to the mean thickness of the snowfall between both radar campaigns, which was corrected accordingly. The radar-retrieved ice thickness data have an error that depends on the vertical resolution of the radar and the uncertainties in RWV and travel time. We calculated this error at each GPR data point of Ariebreen following a technique similar to that described by Navarro & Eisen (2010). The corresponding root mean-square errors of the ice thickness are $\varepsilon_{\mathrm{GPR200}} = 0.66$ m and $\varepsilon_{\mathrm{GPR25}} = 3.46$ m, for the 200-MHz and 25-MHz GPR data, respectively. From the original bias-corrected ice thickness data, we interpolated the ice thickness map using the Kriging method, on the same 20 m $\times$ 20 m regular grid as all other DTMs, giving an interpolation error $\varepsilon_{H\ \mathrm{interp}} = 3.12$ m. As done with the surface DTMs, in practice it can be assumed that the errors $\varepsilon_{\mathrm{GPR}}$ and $\varepsilon_{H\,\mathrm{interp}}$ are independent, and can therefore be combined as the root of their squared summation to give a characteristic error for the ice thickness map that, in the case of Ariebreen, was $\varepsilon_H = 3.29$ m.

We also constructed a subglacial bedrock map subtracting the 2007 ice thickness DTM from the 2007 glacier surface DTM. Its associated error can be obtained from those of their independent error sources through the root of their squared summation, giving $\varepsilon_B = 3.44$ m.

Surface elevation change, elevation change rate and elevation change acceleration maps. The maps of surface elevation change were constructed by subtracting the corresponding DTMs, all of which are built on a common grid 20 m $\times$ 20 m. However, this operation required two preparation steps, as follows. (1) As the glacier extent was different for the distinct years, all DTMs were completed, beyond the glacier limits, up to a rectangle enclosing the largest glacier extent (1936). The ice-free terrain points were taken from the 1990 DTM, except those of the area deglaciated during 1990–2007, which were surveyed by us in 2007 using differential GPS (carrier-phase measurements). (2) We also corrected for terrain uplift due to post-glacial rebound or present-day ice melting. Employing the estimates by Sato et al. (2006) and Kierulf et al. (2009), we took an average uplift rate of 0.005 m y^{-1}. As the 1936 map was already bias-corrected using ground control points measured in 2007, this correction was not necessary. However, the 1990 map used ground control points measured in 1995, so we corrected the 1990–2007 surface elevation change map by the estimated uplift for the period 1995–2007, even if this was a small bias.

As the errors for each DTM are independent, the error in surface elevation change, $\varepsilon_{\Delta Z}$, is given by the root of the squared summation of the errors of the DTMs involved.

The elevation change rate maps for 1936–1990 and 1990–2007 were obtained from the corresponding surface elevation change maps and dividing by the number of years in the period considered. The map of the acceleration of elevation change was calculated as the difference between the elevation change rates for the periods 1936–1990 and 1990–2007, divided by the time between the centres of each period.

Computation of planar area, ice volume (2007), and area and volume changes

We used Surfer software (version 8) to calculate the planar area of Ariebreen in the different years from the corresponding DTMs, the volume in 2007 from the ice thickness map, and the volume change from the surface elevation changes between the different DTMs. For the volume change computation, we used Simpson's numerical integration method. These calculations involve both systematic errors (biases), which we corrected for, and various random errors, including the uncertainty on boundary delineation. The description of how all of these errors were estimated is given in the Supplementary File.

Mass balance rates: 1936–1990 and 1990–2007

Using the geodetic approach, the mean mass balance rate (Cogley et al. 2011) during a period Δt (integer number of mass balance years) is given by

$$\overline{\dot{M}} = \frac{\rho\ \overline{\Delta z}}{\Delta t}, \qquad (1)$$

Citation: *Polar Research* 2013, *32*, 11068, http://dx.doi.org/10.3402/polar.v32i0.11068

where ρ is the density of ice, $\overline{\Delta z} = \Delta V/\bar{A}$ is the mean elevation change, ΔV is the volume change and $\bar{A}$ is the average glacier area (mean value between initial and final areas). Equation 1 assumes Sorge's Law (Bader 1954): that there is no changing firn thickness or density through time and that all volume changes are of glacier ice. This is a reasonable assumption in the case of Ariebreen, since most of the volume changes occur at lower elevations, below the equilibrium-line altitude, and therefore involve ice rather than firn. However, to account for a possible decrease in firn thickness, we took for the density a value of $\rho = 850$ kg m^{-3}, slightly biased towards lower values as compared to usual ice density, and assumed a value of $\varepsilon_\rho = 50$ kg m^{-3} for its error (Huss et al. 2009).

The error in mean mass balance rate is estimated as

$$\varepsilon_{\overline{\dot{M}}} = \frac{1}{\Delta t}\sqrt{\rho^2 \varepsilon^2_{\overline{\Delta z}} + \overline{\Delta z}^2 \varepsilon^2_\rho}, \qquad (2)$$

where we computed the error in mean glacier elevation change $\varepsilon_{\overline{\Delta z}}$ as the error of the quotient $\Delta V/\bar{A}$.

Results

Surface topography 1936, 1990 and 2007, ice thickness 2006–07 and subglacial relief maps

The surface topography in 1936, 1990 and 2007, the ice thickness in 2006–07 and the subglacial relief maps are shown in Figs. 2 and 3. The average ice thickness in 2007 was very low at 27.2 ± 1.6 m. The thickest ice in Ariebreen, 82.3 ± 3.7 m, is found at its upper part. In the middle elevations it rarely exceeds 50 m, while the lower part of the glacier contains rather thin ice (< 30 m).

Area, surface elevation, volume and mass balance changes 1936–1990–2007

The planar area and ice volume of Ariebreen in 1936, 1990 and 2007, together with their percent changes over the periods 1936–1990, 1990–2007 and 1936–2007, are shown in Table 1. Significant changes are observed for both area and volume. Figure 3c shows the surface elevation changes experienced by the glacier over the entire period 1936–2007. The glacier thinning is remarkable, reaching values up to 100 m (ca. 1.4 m y^{-1}) in the lower part of the glacier. To stress the different rates of mass loss over the periods 1936–1990 and 1990–2007, we present, in Fig. 4, the spatial distribution of the elevation change rates for both periods and, in Table 2, the corresponding mean mass balance rates. Note that the elevation change rates in Fig. 4a and b are given in metres of ice per year, while the mass balances in Table 2 are converted into metres in water equivalent (w.eq.) and computed over the average area for the period. Table 2 clearly shows that the mass loss has accelerated during the two last decades, while Fig. 4c shows the spatial distribution of this acceleration by displaying the elevation change acceleration between

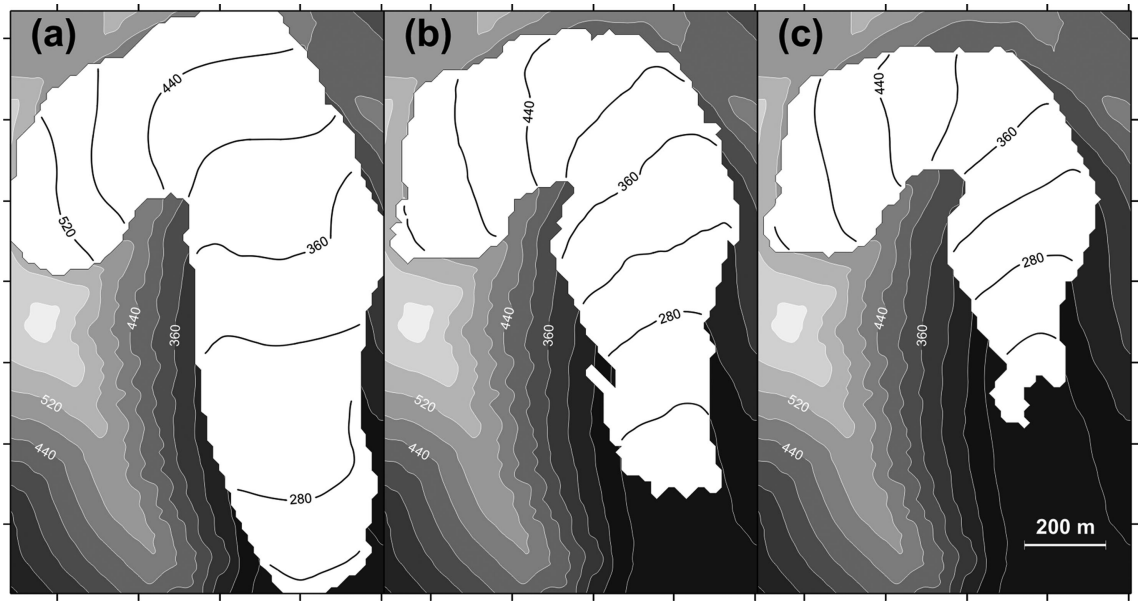

Fig. 2 Surface topography of Ariebreen in (a) 1936, (b) 1990 and (c) 2007. Contour line interval is 40 m. The estimated errors in surface elevation are 13.60, 3.00 and 1.03 m, respectively.

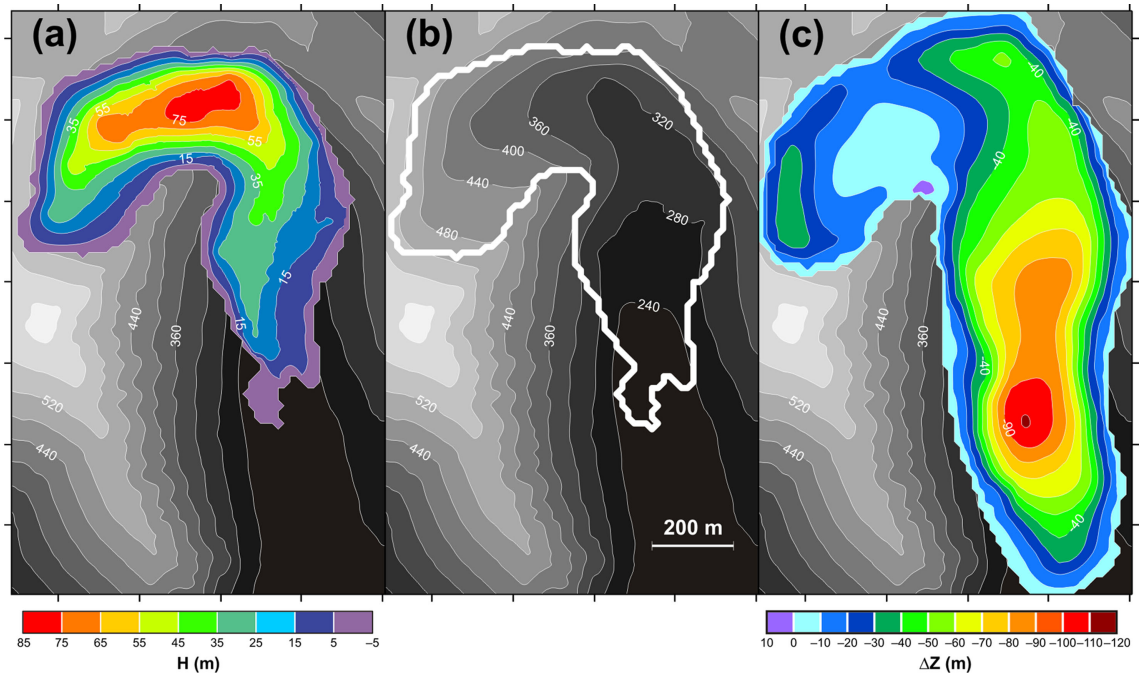

Fig. 3 (a) Map of ice thickness, *H*, of Ariebreen in 2006/07, determined from the radar profiles shown in Fig. 1. Contour line interval is 10 m. The estimated glacier-averaged error in ice thickness is 3.29 m. (b) Bedrock topography of Ariebreen, determined by subtracting the ice thickness shown in Fig. 3 from the surface topography shown in Fig. 2c. Contour line interval is 40 m. The estimated error in bedrock elevation is 3.44 m. (c) Map of surface elevation changes, ΔZ, of Ariebreen during the period 1936–2007. Negative values mean thinning. Contour line interval is 10 m. The estimated error is 13.64 m.

the centres of each of the two periods 1936–1990 and 1990–2007.

Radar results concerning the internal structure of the glacier

The analysis of the radar sections (two examples are provided in Fig. 5) shows two main features concerning the internal structure of Ariebreen: (1) the radar records of both high- (200 MHz) and low- (25 MHz) frequency radars do not show any englacial diffractors or scattering typical of temperate ice; (2) the firn layer observed in the field measurements, whose approximate extent is shown by the equilibrium line positions in Fig. 1, cannot be detected in our radar records because the 200-MHz profile on the upper glacier does not penetrate into the accumulation area (see Fig. 1), and the uppermost 6–8 m of the 25-MHz data are obscured by the direct waves.

Discussion

Hydrothermal structure of Ariebreen

The radar data suggest that Ariebreen is entirely cold. This is not surprising, given that the relatively thin ice is not sufficient to prevent conduction of geothermal and internal heat fluxes, that the slow dynamics implies little strain heating, and that the limited extent and thickness of the firn area implies a reduced penetration of percolating water and the release of latent heat upon refreezing. Nevertheless, Ariebreen was classified in the past as a polythermal glacier (Jania 1988), on the basis of occasional observations of water outflows during winter time and proglacial icings. This, however, is no longer so widely accepted as an indication that the glacier is polythermal (e.g., Hodgkins et al. 2004; Bælum & Benn 2011).

Table 1 Glacier area and volume of Ariebreen in 1936, 1990 and 2007, and their percent changes for the different periods.

				% change		
	1936	1990	2007	1990/1936	2007/1990	2007/1936
Area (km^2)	0.700±0.070	0.519±0.016	0.374±0.008	−25.9±10.3	−28.0± 3.4	−46.6± 10.1
Volume (km^3)	0.0374±0.0044	0.0186±0.0009	0.0102±0.0006	−52.2±12.0	−45.4±4.1	−72.8±11.7

Citation: *Polar Research* 2013, *32*, 11068, http://dx.doi.org/10.3402/polar.v32i0.11068

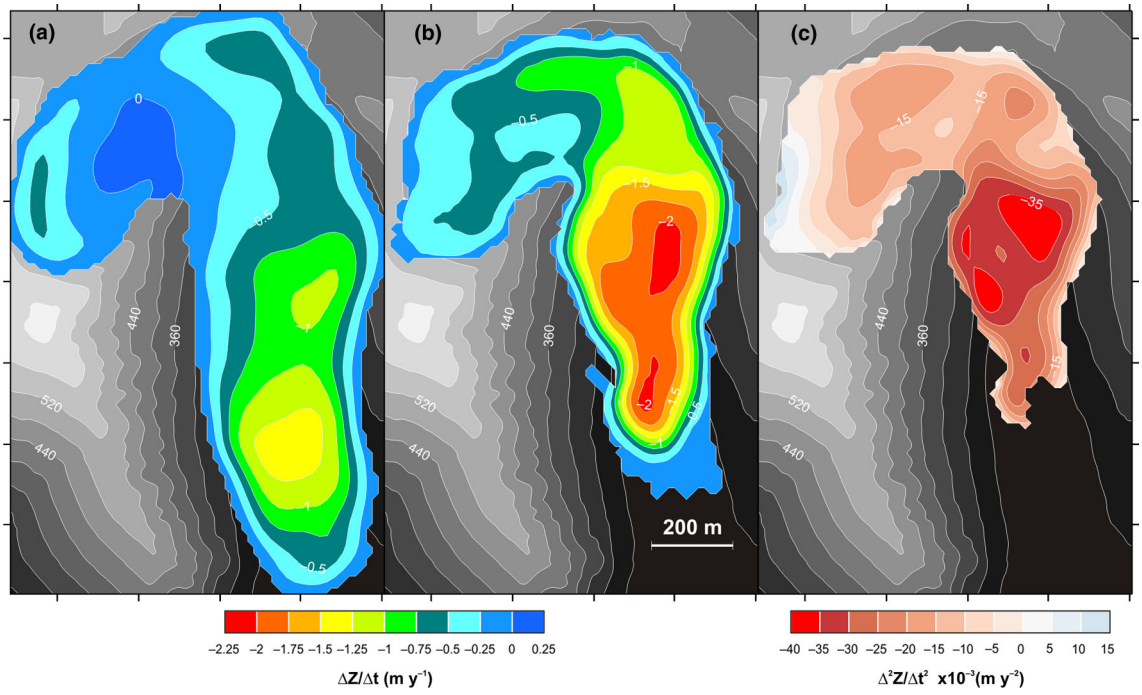

Fig. 4 Spatial distribution of the elevation change rate, $\Delta Z/\Delta t$, of Ariebreen for the periods (a) 1936–1990 and (b) 1990–2007, respectively. Contour line interval is 0.25 m y^{-1}. (c) Spatial distribution of the elevation change acceleration, $\Delta^2 Z/\Delta t^2$, between both periods, computed as the increment of elevation change rate divided by the time between the centres of each period. The estimated errors are 0.26, 0.19 m y^{-1} and 0.009 m y^{-2}, respectively. The quantities are not converted to water equivalent.

Comparison of the mean mass balance rate with other regional studies

According to our results, during the period 1936–1990 the area of Ariebreen decreased by 26%, and the mean mass balance rate was -0.50 ± 0.22 m y^{-1} w.eq. For comparison, the results by Nuth et al. (2007) for Wedel Jarlsberg Land during the same period were a decrease of the glacierized area by 12%, and a mean mass balance rate of -0.39 ± 0.02 m y^{-1} w.eq. Ariebreen has therefore followed the regional pattern of changes, though at a larger rate. We attribute these enhanced losses to the small thickness of Ariebreen, which implies a short response time to changes in climate. The estimates of the mean mass balance rate of Svalbard by Hagen and co-workers (Hagen, Kohler et al. 2003; Hagen, Melvold et al. 2003) are even smaller in magnitude, -0.27 and -0.12 m y^{-1} w.eq., obtained using two different methods and data from the late 1960s to about 2000. However, this discrepancy arises because the north and north-eastern regions of Svalbard studied by Hagen and co-workers are less negative than the southern and western regions.

Table 2 Mean mass balance rate equivalent to the volume changes of Ariebreen estimated from surface elevation changes over different periods.

	1936–1990	1990–2007	1936–2007
Mean mass balance rate (m y^{-1} w.eq.)	-0.50 ± 0.22	-0.95 ± 0.17	-0.61 ± 0.17

During the second period analysed (1990–2007), our data show a mean mass balance rate of -0.95 ± 0.17 m y^{-1} w.eq., which can be compared to the -0.65 ± 0.08 m y^{-1} w.eq. estimated by Nuth et al. (2010) for Wedel Jarlsberg Land and a similar period (1990–2005). However, the mass losses experienced by Ariebreen are larger than the regional values.

The negative mean mass balance rate of Ariebreen has nearly doubled between the two periods analysed. This marked acceleration of the mass losses is consistent with the regional trend, but at a larger rate than the regional value. This acceleration is apparent comparing the maps of elevation change rates for the periods 1936–1990 and 1990–2007 (Fig. 4a, b), as well as in the map of elevation change acceleration (Fig. 4c).

Spatial distribution of the elevation change rate

Figure 4a and b show the spatial distribution of the elevation change rates for the periods 1936–1990 and 1990–2007, respectively, where nearly ubiquitous thinning is observed. During the earlier period, the largest thinning is shown between 260 and 360 m of altitude, and

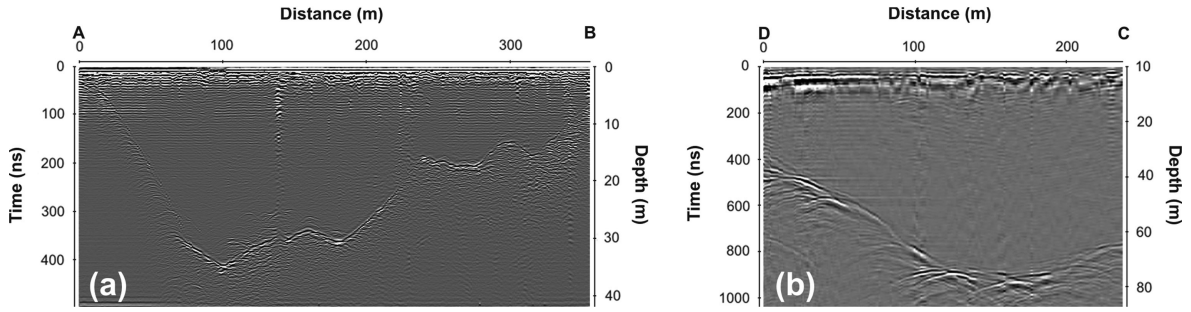

Fig. 5 Examples of radar sections: (a) 200-MHz radar, corresponding to a transverse profile on the lower glacier (profile A–B in Fig. 1); (b) 25-MHz radar, corresponding to a transverse profile on the upper glacier (profile C–D in Fig. 1). Both are free from the internal diffractions and scattering typical of temperate ice.

approaches zero at ca. 420 m in the shadowed area of the cirque. Although at the upper elevations a limited zone shows a slight thickening (see Fig. 4a), this is not significant due to the rather large error of the map, stemming from the error of the 1936 DTM. This pattern of changes agrees with that observed in the regional study by Nuth et al. (2007), who pointed out that, during 1936–1990, the elevation losses were largest at the lower elevations, while the upper elevations slightly thickened, and is also consistent with other studies in the area (Bamber et al. 2004; Bamber et al. 2005). During 1990–2007, the thinning spanned the full altitude range of Ariebreen, though it was still more pronounced at the lower elevations. The changes at the upper elevations involve a switch from near-equilibrium conditions in 1936–1990 to clear thinning conditions in 1990–2007. Our elevation change rates for the latter period agree with the statement by Nuth et al. (2010) that, at higher elevations, Svalbard glaciers are generally thinning at rates from -0.1 to -1 m y^{-1}.

The likely reasons why the thinning rates of Ariebreen are largest at the lower elevations, and larger than the regional averages, are: (1) the morphology of Ariebreen, whose tongue is orientated towards the south and well exposed to solar radiation, while its upper part is largely shadowed, reducing melting by radiation; (2) the very low ice velocities of Ariebreen (maximum of ca. 1.6 m y^{-1}). On a more active glacier, the ice motion would replenish the ice lost by melting at the lower parts and the actual thinning would be less. However, on Ariebreen, with very low ice speeds, a large part of the melting would result in a surface lowering and the thinning rate would become higher.

Spatial distribution of the elevation change acceleration

As shown in Fig. 4c, the acceleration of elevation change has been largest in the mid-lower elevations, which differs from the observation by Kohler et al. (2007) and by James et al. (2012) that the thinning acceleration on the upper parts of their studied glaciers is larger or similar to that measured in the lower part. We first note that the glaciers that they studied are located in other Svalbard regions (northern and central Spitsbergen, and Edgeøya) and span elevation ranges different from that of Ariebreen. Second, both Kohler et al. (2007) and James et al. (2012) argue that changes in albedo will more strongly influence the response higher upglacier as surfaces there change from snow to bare ice, for instance as a consequence of a trend towards less winter accumulation. However, such a trend has not been reported for Ariebreen region. These arguments could explain the different behaviour of Ariebreen. Nevertheless, if we take into account the low quality of the 1936 map, based on oblique photography, the actual poor camera views towards Ariebreen when mapping its upper reaches, and the difficulties of mapping snow-covered areas, then our observation of higher accelerations at the upper reaches of Ariebreen cannot be established as a firm conclusion.

Conclusions

The following main conclusions can be drawn from our analysis.

Ariebreen has experienced a significant shrinkage since 1936, involving both glacier thinning and retreat of its front. During the period 1936–2007, its area has decreased by $47 \pm 10\%$.

During the period 1936–2007, the ice volume of the glacier decreased by $73 \pm 12\%$. This is equivalent to a mean mass balance rate of -0.61 ± 0.17 m y^{-1} w.eq.

During 1936–1990, the thinning focused on the lower elevations, with negligible surface elevation changes at the upper part of the glacier, while during 1990–2007 the thinning was widespread, though still more marked at the lower elevations.

Citation: *Polar Research* 2013, *32*, 11068, http://dx.doi.org/10.3402/polar.v32i0.11068

There has been a marked acceleration of the mass losses during the two last decades, from a mean mass balance rate of -0.50 ± 0.22 m y^{-1} w.eq., for the period 1936–1990, to -0.95 ± 0.17 m y^{-1} w.eq. for the period 1990–2007. The corresponding acceleration of elevation changes spans the full altitude range of Ariebreen. Although our data suggest that the acceleration has been larger at the middle-lower elevations as compared with the cirque, the poor quality of the 1936 map does not allow us to firmly assert it.

Ariebreen is an entirely cold glacier, with a firn layer thinner than 6–8 m.

Acknowledgements

This research was supported by grants CGL2005–05483 and CTM2008-05878 from the Spanish Ministries of Education and Science and Science and Innovation, respectively, and NCBiR/PolarCLIMATE-2009/2-2/2010 and N N306 094939 from the Polish National Centre for Research and Development and the Polish Ministry of Science and Higher Education, respectively. The authors thank the crew of Hornsund Polish Polar Station for their support to our fieldwork. They also thank Subject Editor Jack Kohler, the reviewer Christopher Nuth and two anonymous reviewers for their many suggestions to improve the manuscript.

References

Bader H. 1954. Sorge's Law of densification of snow on high polar glaciers. *Journal of Glaciology 2*, 319–323.

Bælum K. & Benn D.I. 2011. Thermal structure and drainage system of a small valley glacier (Tellbreen, Svalbard), investigated by ground penetrating radar. *The Cryosphere 5*, 139–149.

Bamber J., Krabill W., Raper V. & Dowdeswell J. 2004. Anomalous recent growth of part of a large Arctic ice cap: Austfonna, Svalbard. *Geophysical Research Letters 31*, L12402, doi: 10.1029/2004GL019667.

Bamber J.L., Krabill W., Raper V., Dowdeswell J.A. & Oerlemans J. 2005. Elevation change measured on Svalbard glaciers and ice caps from airborne laser data. *Annals of Glaciology 42*, 202–208.

Cogley J.G., Hock R., Rasmussen L.A., Arendt A.A., Bauder A., Braithwaite R.J., Jansson P., Kaser G., Möller M., Nicholson L. & Zemp M. 2011. *Glossary of glacier mass balance and related terms. IHP-VII Technical Documents in Hydrology 86. IACS Contribution 2*. Paris: United Nations Educational, Scientific and Cultural Organization.

Cuffey K.M. & Paterson W.S.B. 2010. *The physics of glaciers.* 4th edn. Oxford: Elsevier.

Hagen J.O., Kohler J., Melvold K. & Winther J.G. 2003. Glaciers in Svalbard: mass balance, runoff, and freshwater flux. *Polar Research 22*, 145–159.

Hagen J.O., Liestøl O., Roland E. & Jørgensen T. 1993. *Glacier atlas of Svalbard and Jan Mayen. Norsk Polarinstittut Meddelelser 129*. Oslo: Norwegian Polar Institute.

Hagen J.O., Melvold K., Pinglot F. & Dowdeswell J.A. 2003. On the net mass balance of the glaciers and ice caps in Svalbard, Norwegian Arctic. *Arctic, Antarctic and Alpine Research 35*, 264–270.

Hodgkins R., Tranter M. & Dowdeswell J.A. 2004. The characteristics and formation of a High-Arctic proglacial icing. *Geografiska Annaler Series A 86*, 265–275.

Huss M., Bauder A. & Funk M. 2009. Homogenization of long-term mass-balance time series. *Annals of Glaciology 50*, 198–206.

Hutchinson M.F. 1989. A new procedure for gridding elevation and stream line data with automatic removal of spurious pits. *Journal of Hydrology 106*, 211–232.

James T.D., Murray T., Barrand N.E., Sykes H.J., Fox A.J. & King M.A. 2012. Observations of enhanced thinning in the upper reaches of Svalbard glaciers. *The Cryosphere 6*, 1369–1381.

Jania J. 1988. *Dynamiczne procesy glacjalne na poludniowym Spitsbergenie (w swietle badan fotointerpretacyjnych i fotogrametrycznych). (Dynamic glacial processes in southern Spitsbergen [in the light of photointerpretation and photogrammetric research].)* (In Polish with English summary.) Katowice, Poland: University of Silesia.

Jania J., Kolondra L. & Aas H.F. (eds.) 2002. *Werenskioldbreen and surrounding areas. Spitsbergen, Svalbard, Norway. Orthophotomap 1:25000*. Katowice, Poland: University of Silesia and Tromsø, Norwegian Polar Institute.

Jania J., Macheret Y.Y., Navarro F.J., Glazovskiy A.F., Vasilenko E.V., Lapazaran J., Glowacki P., Migala K., Balut A. & Piwowar B.A. 2005. Temporal changes in the radiophysical properties of a polythermal glacier in Spitsbergen. *Annals of Glaciology 42*, 125–134.

Kierulf H.P., Plag H.-P. & Kohler J. 2009. Surface deformation induced by present-day ice melting in Svalbard. *Geophysical Journal International 179*, 1–13.

Kohler J., James T.D., Murray T., Nuth C., Brandt O., Barrand N.E., Aas H.F. & Luckman A. 2007. Acceleration in thinning rate on western Svalbard glaciers. *Geophysical Research Letters 34*, L18502, doi: 10.1029/2007GL030681.

Kolondra L. 2002. Cyfrowa ortofotomapa—nowa forma danych kartograficznych w badaniach glacjologicznych (na przykladzie lodowców Werenskiold i Nann—S Spitsbergen). (Digital orthophotomap—a new form of cartographic data for glaciological studies [an example of Werenskiold and Nann glaciers, southern Spitsbergen].) In A. Kostrzewski & G. Rachlewicz (eds.): *Polish polar studies. Funkcjonowanie i monitoring geoekosystemów obszarów polarnych. (The operation and monitoring of geosystems of polar areas.)* Pp. 173–186. Poznan, Poland: Bogucki Scientific Publishers.

Kuziemski J. 1968. Hydrological conditions in the vicinity of the Polish Base at Isbjornhamna, Hornsund 1958. In

K. Birkenmajer (ed.): *Polish Spitsbergen expeditions 1957–1960, summary of scientific results*. Pp. 67–75. Warsaw: Wydawnictwa Geologiczne.

Navarro F.J. & Eisen O. 2010. Ground penetrating radar. In P. Pellikka & W.G. Rees (eds.): *Remote sensing of glaciers—techniques for topographic, spatial and thematic mapping*. Pp. 195–229. Leiden, The Netherlands: CRC Press/Balkema.

Norwegian Polar Institute. 1953. *1:100 000 Svalbard topographic map. Sheet B12 Torellbreen.* Oslo: Norwegian Polar Institute.

Nuth C., Kohler J., Aas H.F., Brandt O. & Hagen J.O. 2007. Glacier geometry and elevation changes on Svalbard (1936–90): a baseline dataset. *Annals of Glaciology 46*, 106–116.

Nuth C., Moholdt G., Kohler J., Hagen J.O. & Kääb A. 2010. Svalbard glacier elevation changes and contribution to sea level rise. *Journal of Geophysical Research—Earth Surface 115*, F01008, doi: 10.1029/2008JF001223.

Pälli A., Moore J.C., Jania J., Kolondra L. & Glowacki P. 2003. The drainage pattern of Hansbreen and Werenskioldbreen, two polythermal glaciers in Svalbard. *Polar Research 22*, 355–371.

Sato T., Okuno J., Hinderer J., MacMillan D.S., Plag H.-P., Francis O., Falk R. & Fukuda Y. 2006. A geophysical interpretation of the secular displacement and gravity rates observed at Ny-Alesund, Svalbard in the Arctic: effects of post-glacial rebound and present-day ice melting. *Geophysical Journal International 165*, 729–743.

Werner A. 1993. Holocene moraine chronology, Spitsbergen, Svalbard: lichenometric evidence for multiple Neoglacial advances in the Arctic. *The Holocene 3*, 128–137.

Citation: *Polar Research* 2013, *32*, 11068, http://dx.doi.org/10.3402/polar.v32i0.11068